Dr. MONISHA CHAKRABORTY/ International Journal of Engineering Research and Applications (IJERA) ISSN: 2248-9622 www.ijera.com

Vol. 1, Issue 4, pp.2096-2104

A STUDY OF DIMENSIONAL EFFECT ON STRUCTURAL PROPERTIES OF CADMIUM ZINC TELLURIDE THIN FILMS

Dr. MONISHA CHAKRABORTY

Assistant Professor, School of Bio-Science & Engineering, Jadavpur University, 188, Raja S. C. Mallik Road, Kolkata-700032, India.

ABSTRACT

In this work, thin films of $Cd_{1-x}Zn_xTe$ of 1µm and 100nm thickness are fabricated on plain glass substrates with 'x' varying from 0.0567 to 0.2210. Structural properties of these $Cd_{1-x}Zn_xTe$ 1µm and 100nm thin films are studied. The structural properties of these fabricated films are found to be functions of film thickness and 'x'. The present paper has dealt with the estimation of dimensional effect on $Cd_{1-x}Zn_xTe$ thin films in the light of structural characterization studies.

Keywords - $Cd_{1-x}Zn_xTe$, Dimensional effect, Film thickness, Structural characterization, Thin films.

1. Introduction

II-VI semiconductor compounds e.g. ZnTe, CdTe and their alloys $Cd_{1-x}Zn_xTe$ with stoichiometric value 'x', are the materials of choice for infrared detectors, solar cells and other optoelectronic devices [1-5]. Due to their chemical and structural compatibility, they are also used as substrates for growing epitaxial layers of HgCdTe, a useful IR detecting material in the 8–12 mm infrared range. Introduction of Zn into CdTe makes the lattice of $Cd_{1-x}Zn_xTe$ tunable and by adjusting the Cd/Zn ratio, a lattice-matched substrate for the growth of the HgCdTe epitaxial layer has been reported in [6]. Designable semiconductor band gap is helpful for controlling the resistivity as well as the valence and conduction band alignment at the semiconductor interface. Owing to extensive research and industrial work conducted by teams of solid-state physicists, engineers and medical physicists, CdTe/CZT detectors are now widely used. CdTe/CZT-based surgery probes have large impact on patient management in surgical oncology. Excellent large-field of view modules have already been realized as reported in [7]. The performance of a CZT dual Positron Emission Tomography (PET), dedicated for breast cancer, is studied by a group of researchers and these are reported in [8]. Studies in [9] report on dedicated emission mammotomography with CZT imaging detector. A comprehensive review of the material properties of $Cd_{1-x}Zn_xTe$ with varying zinc content is reported in [10]. Some studies on the structural and optical properties of II-VI compound semiconductors are proposed previously and these are reported in [11-20]. The range of 'x' in $Cd_{1-x}Zn_xTe$ lies preferably within $0.05 \leq$ 'x' ≤ 0.95 [19, 21].

In the present work, $Cd_{1-x}Zn_xTe$ thin films of 1µm and 100nm thickness for 'x' varying from 0.0567 to 0.2210 are fabricated on plain glass substrates. These films are subjected to structural characterization studies. The method to determine strain and particle size from XRD analysis has been repoted in [22-23]. In the present paper, the variation of strain with partice size for $Cd_{1-x}Zn_xTe$ 1µm and 100nm thin films are obtained. Film properties are found to change with the change in the thickness of the film.

In this work, proper methods are adopted to fabricate $Cd_{1-x}Zn_xTe$ thin films of 1µm and 100nm thickness and these are discussed in section 2 of this paper. The mathematical calculation for obtaining experimentally designed value of 'x' is discussed in section 2.1 of this paper. The structural characterization results of $Cd_{1-x}Zn_xTe$ thin films of 1µm and 100nm thickness are discussed in section 3 of this paper. Particle size and strain for $Cd_{1-x}Zn_xTe$ 1µm and 100nm thin films are obtained from XRD results and these are discussed in section 3.1 of this paper. The significance of the results of this work is discussed with respect to dimensional effect in section 4 of this paper. The work is concluded in section 5 of this paper.

2. Materials and Methods

In this work, physical deposition method is adopted to fabricate large area $Cd_{1-x}Zn_xTe$ thin films of 1µm and 100nm thickness. Surface cleaning of the substrate has predominant effect on the growth of the film on it. Thus prior to deposition, glass substrates are carefully cleaned. Commercially available glass slides of

dimensions 23 mm x 37 mm x 1 mm are dipped in chromic acid for two hours. These are washed with detergent and finally ultrasonically cleaned with acetone before use.

In order to design the six different compositions of $Cd_{1-x}Zn_xTe$ thin films of 1µm and 100nm thickness, six different % ratio of the stack layer of ZnTe/CdTe is chosen and these are 20:80, 30:70, 40:60, 50:50, 60:40 and 70:30. For these six ratios of the stack layer of ZnTe/CdTe, six different values of 'x' are obtained. The mathematical detail is discussed with a sample calculation in section 2.1 of this paper.

For the film fabrication, 500W RF Sputtering unit has been used. ZnTe and CdTe targets are placed in the target holders of the RF sputtering unit. Plain glass substrates are kept at the bottom of the target holder and temperature to the order of 100°C is maintained on the substrates. Argon gas is injected from outside and pressure of the order of 10^{-2} Torr has been maintained. At this pressure, the RF unit is energized and a power of 500W with a frequency of 13.56 MHz is applied between the target and the substrate. On application of this RF power the target gets energized and vapour of the target material produced deposits on the substrate. At the substrate temperature the film gets crystallized and the thickness is dependent on the sputtering time. Both CdTe and ZnTe targets are sputtered sequentially and a stack layer of ZnTe/CdTe is thus obtained. The stack layer is then annealed in vacuum (10^{-5} Torr) for an hour at 300°C. Both Cadmium and Zinc tried to inter-diffuse among each other to get into a stabilized state. Applications of thermal energy initiate both cadmium and zinc inter-diffusion. However, the stoichiometric ratio of cadmium and zinc is not equal and as a result the film is formed in the form of $Cd_{1-x}Zn_xTe$. The value of 'x' decides whether the film is CdTe or ZnTe. Thickness and deposition time for CdTe and ZnTe layers for each composition of $Cd_{1-x}Zn_xTe$ thin films of 1µm thickness are tabulated in Table 1(a). Similarly, thickness and deposition time for CdTe and ZnTe layers for each composition of $Cd_{1-x}Zn_xTe$ 100nm thin films are tabulated in Table 1(b)

Table 1(a) Thickness and Deposition Times of ZnTe and CdTe layers in 1µm CZT Films

S..No.	(%ZnTe):(%CdTe)	Thickness of ZnTe layer T_{ZnTe} (nm)	Thickness of CdTe layer T_{CdTe} (nm)	Deposition time of CdTe layer t_{CdTe}	Deposition time of ZnTe layer t_{ZnTe}	Fraction of Zinc in CZT matrix, 'x'
1	20:80	156.48	843.52	10 mins 49 sec	3 mins 29 sec	0.0567
2	30:70	241.29	758.71	9 mins 44 sec	5 mins 22 sec	0.0870
3	40:60	330.97	669.03	8 mins 35 sec	7 mins 21 sec	0.1182
4	50:50	425.95	574.05	7 mins 22 sec	9 mins 28 sec	0.1510
5	60:40	526.74	473.26	6 mins 4 sec	11 mins 42 sec	0.1865
6	70:30	633.88	366.12	4 mins 42 sec	14 mins 5 sec	0.2210

Table 1(b) Thickness and Deposition Times of ZnTe and CdTe layers in 100 nm CZT Films

S.No.	(%ZnTe):(%CdTe)	Thickness of ZnTe layer T_{ZnTe} (nm)	Thickness of CdTe layer T_{CdTe} (nm)	Deposition time for CdTe layer t_{CdTe}	Deposition time for ZnTe layer t_{ZnTe}	Fraction of Zinc in CZT matrix, 'x'
1	20:80	15.65	84.35	1 min 5 sec	21 sec	0.0567
2	30:70	24.13	75.87	58 sec	32 sec	0.0870
3	40:60	33.10	66.90	51 sec	44 sec	0.1182
4	50:50	42.60	57.40	44 sec	57 sec	0.1510
5	60:40	52.67	47.33	36 sec	1 min 10 sec	0.1865
6	70:30	63.39	36.61	28 sec	1 min 25 sec	0.2210

2.1. Sample Calculation of 'x'

In this section, the mathematics to determine 'x' in $Cd_{1-x}Zn_xTe$ film is discussed with a sample calculation. For this purpose, one out of the six samples is considered and this is a 1µm stack of CZT comprised

of ZnTe film deposited on CdTe film. Percentage thickness ratio of ZnTe : CdTe layer is 60:40 and this can be expressed as given in Eq. (1.1).

$$\frac{\%ZnTe}{\%CdTe} = \frac{60}{40} = \frac{n_{ZnTe}}{n_{CdTe}} = \frac{\frac{m_{ZnTe}}{M_{ZnTe}}}{\frac{m_{CdTe}}{M_{CdTe}}} \quad (1.1)$$

where,

m_{ZnTe} and m_{CdTe} are the masses of ZnTe and CdTe layers respectively to attain the % ratio ZnTe : CdTe as 60:40. M_{ZnTe} and M_{CdTe} are the molar masses of ZnTe and CdTe respectively and these values are M_{ZnTe} =193 gms/mol and M_{CdTe}=240 gms/mol. On putting these values, Eq. (1.1) becomes,

$$1.5 = \frac{\rho_{ZnTe}.T_{ZnTe}.A.240}{\rho_{CdTe}.T_{CdTe}.A.193} \quad (1.2)$$

where,

'A' is the cross-sectional area of the substrate. ρ_{ZnTe} and ρ_{CdTe} are the density of ZnTe and CdTe layers respectively and these values are ρ_{ZnTe} = 6.34 gms/cc and ρ_{CdTe}=5.85 gms/cc. T_{ZnTe} and T_{CdTe} are the values of thickness of ZnTe and CdTe layers respectively. On putting these values, Eq. (1.2) becomes,

$$\frac{T_{ZnTe}}{T_{CdTe}} = 1.113022477 \quad (1.3)$$

$$T_{ZnTe} + T_{CdTe} = 1\mu m \quad (1.4)$$

Solution of Eq. (1.3) and Eq. (1.4) gives the values of the thickness of CdTe and ZnTe layers and these are,

T_{CdTe} = 473.26 nm and T_{ZnTe} = 526.74 nm. (1.5 a)

Deposition rates for CdTe and ZnTe targets are 78 nm/min and 45 nm/min respectively. (1.5 b)

From Eq. (1.5 a) and Eq. (1.5 b) the deposition times for CdTe and ZnTe layers for this sample are obtained and these values are t_{CdTe} = 6 mins 4 sec and t_{ZnTe} = 11 mins 42 sec respectively. (1.5 c)

So, mass of ZnTe layer, $m_{ZnTe} = 3339.53.A.10^{-7}$ gms

and mass of CdTe layer, $m_{CdTe} = 2768.57.A.10^{-7}$ gms.

Molar mass of Zinc, M_{Zn} = 65.38 gms/mol.

So, $1139.29.A.10^{-7}$ gms of zinc is present in $3339.53.A.10^{-7}$ gms of ZnTe.

$$\therefore \text{ Fraction of zinc in this CZT matrix} = \frac{1139.29.A.10^{-7}}{(2768.57+3339.53).A.10^{-7}} = 0.1865 \quad (1.6)$$

Similarly, for other % ratios of ZnTe : CdTe layers for both the thickness domains considered in this study, the values of 'x' are calculated and these results are tabulated in Table 1(a) and Table 1(b).

3. Structural Characterization and Results

X-ray diffraction (XRD) spectra of the films are recorded on Rigaku Miniflex (Japan) powder diffractometer using Cu Kα radiation (1.5406 Å). The scanning angle range, 2θ of the diffractometer, is from 20º to 70º. XRD spectra of $Cd_{1-x}Zn_xTe$ 1μm and 100 nm thin films for the composition at 'x' = 0.1865 are shown in Fig. 1(a) and Fig. 1(b) respectively as sample results.

At constant temperature, crystal lattice constant of an alloy bears a linear relationship with the concentrations of the constituent elements [24]. For a simple cubic lattice, the lattice constant bears a relation with d-value where'd' is the spacing between adjacent parallel planes [25]. So, this implies that the 2θ values of the peaks of $Cd_{1-x}Zn_xTe$ 1μm and 100 nm thin films at 'x' = 0.1865, as shown in Fig. 1 (a) and Fig. 1(b) respectively will lie in between the 2θ values of the peaks of the corresponding planes of CdTe and ZnTe cubic crystals. On the basis of this idea and standard JCPDS files, CZT peaks in the XRD spectra of $Cd_{1-x}Zn_xTe$ 1μm and 100 nm thin films at 'x' = 0.1865 are identified and the details of these results are tabulated in Table 2(a) and Table 3(a) respectively. Peaks other than CZT are also identified in the XRD spectra of $Cd_{1-x}Zn_xTe$ 1μm and 100 nm thin films at 'x' = 0.1865 and the details of these results are tabulated in Table 2(b) and Table 3(b) respectively.

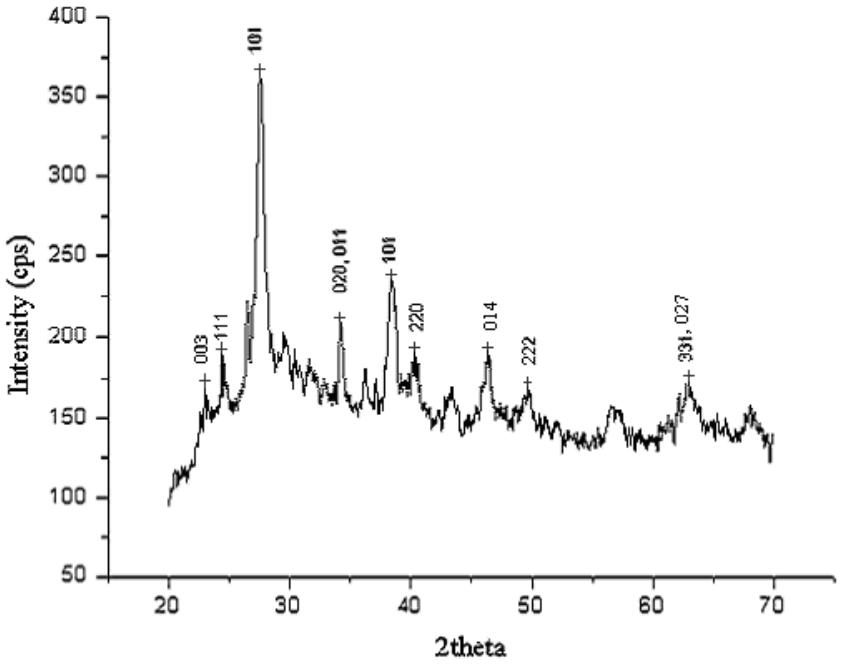

Fig. 1(a) XRD spectra of 1µm $Cd_{1-x}Zn_xTe$ thin film at 'x' = 0.1865

Table 2(a) Details of CZT peaks in $Cd_{1-x}Zn_xTe$ 1µm thin film at 'x' = 0.1865

S. No.	Peak No.	2theta (deg)	I/Io	Planes	JCPDS Card No.
1	5	24.02	14	003	CZT-471296
2	6	24.47	18	111	CdTe-752083-ZnTe-800022
3	15	40.37	26	220	CdTe-752083-ZnTe-800022
4	15	40.37	26	220	CZT-471296
5	21	49.64	18	222	CdTe-752083-ZnTe-752085
6	28	63.62	8	027	CZT-471296
7	28	63.62	8	331	CdTe-752083-ZnTe-800022

Table 2(b) Details of other peaks in $Cd_{1-x}Zn_xTe$ 1μm thin film at 'x' = 0.1865

S. No.	Peak No.	2theta (deg)	I/Io	Planes	JCPDS Card No.
1	8	27.56	100	101	Te-850555
2	13	38.33	33	101	Cd-851328
3	10	35.19	10	020, 011	CdTe-410941
4	19	46.49	15	014	ZnTe-830966

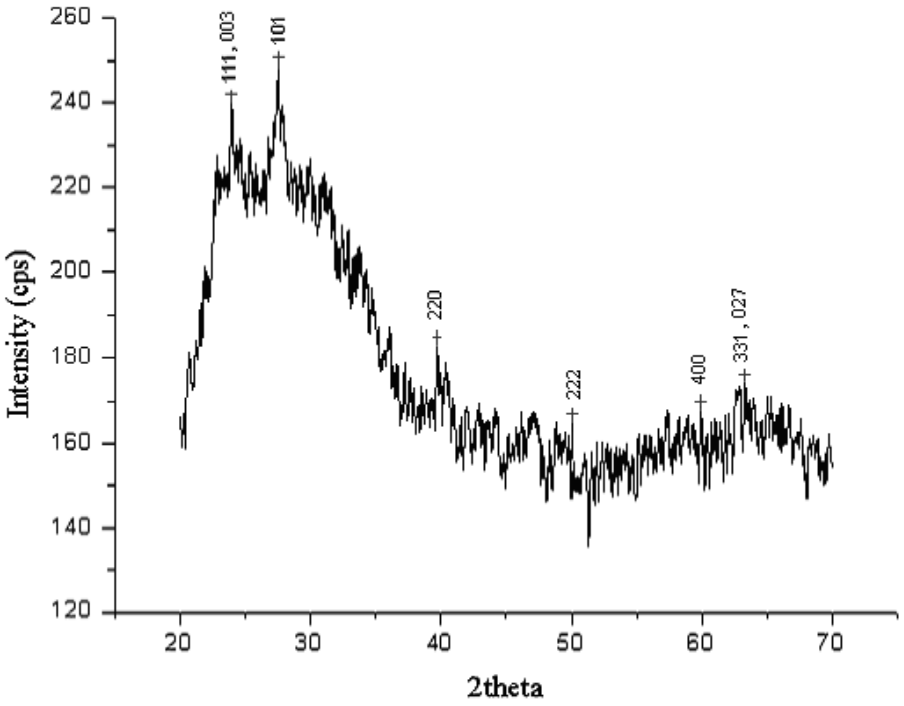

Fig. 1(b) XRD spectra of $Cd_{1-x}Zn_xTe$ 100 nm thin film at 'x' = 0.1865

Table 3(a) Details of CZT peaks in $Cd_{1-x}Zn_xTe$ 100 nm thin film at 'x' = 0.1865

S. No.	Peak No.	2theta (deg)	I/Io	Planes	JCPDS Card No.
1	3	23.93	89	111	CdTe-150770-ZnTe-800022
2	3	23.93	89	003	CZT- 471296
3	10	39.68	62	220	CdTe-150770-ZnTe-800022
4	10	39.68	62	220	CZT- 471296
5	13	49.82	48	222	CdTe-752083-ZnTe-800002
6	16	59.93	58	400	CdTe-752083-ZnTe-800022
7	21	62.93	47	331	CdTe-150770-ZnTe-752085
8	21	62.93	47	027	CZT- 471296

Table 3(b) Details of other peak in $Cd_{1-x}Zn_xTe$ 100 nm thin film at 'x' = 0.1865

S. No.	Peak No.	2theta (deg)	I/Io	Planes	JCPDS Card no
1	6	27.47	100	101	Te-850555

Similarly, for other values of 'x', XRD spectra are obtained for both $Cd_{1-x}Zn_xTe$ 1µm and 100 nm thin films and their respective results have shown good agreement with standard JCPDS files. CZT planes in both $Cd_{1-x}Zn_xTe$ 1µm and 100 nm thin films are thus identified and these are tabulated in Table 4(a) and Table 4(b) respectively. The presence of CZT planes are marked by tick (√) and the absence of these planes are marked as blank in Table 4(a) and Table 4(b).

Table 4(a) Identified CZT planes in $Cd_{1-x}Zn_xTe$ 1µm thin films

Fraction of Zinc (x)	111	003	220	024	311	400	404	222	401	331	027	420
0.0567	√	√	√	√	√	√	√					
0.0870	√	√	√		√			√	√	√	√	
0.1182	√	√	√		√	√		√	√			
0.1510	√	√	√		√	√		√		√	√	
0.1865	√	√	√					√		√	√	
0.2210	√	√	√					√		√		√

Table 4(b) Identified CZT planes in $Cd_{1-x}Zn_xTe$ 100nm thin films

Fraction of Zinc (x)	111	003	200	220	311	400	420	331	027	021	222
0.0567	√	√	√	√	√	√	√				
0.0870	√		√		√		√				
0.1182	√	√	√				√	√	√		
0.1510			√		√	√		√	√		
0.1865	√	√		√		√		√	√		√
0.2210	√			√	√			√		√	√

3.1. Determination of Strain and Particle Size

The FWHM (β) can be expressed as a linear combination of the contributions from the strain (ε) and particle size (L) by Eq. (1.7) [23-24].

$$\frac{\beta\cos\theta}{\lambda} = \frac{1}{L} + \frac{\varepsilon\sin\theta}{\lambda} \qquad (1.7)$$

Plots showing the variation of $\frac{\sin\theta}{\lambda}$ vs $\frac{\beta\cos\theta}{\lambda}$ obtained from $Cd_{1-x}Zn_xTe$ 1μm and 100 nm thin films for the composition at 'x' = 0.1865 are shown in Fig. 2(a) and Fig 2(b) respectively as sample results.

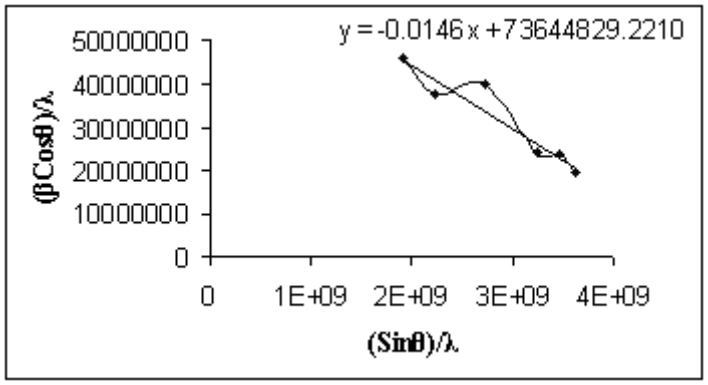

Fig. 2(a) Variation of (Sinθ)/λ vs (βCosθ)/λ of 1μm $Cd_{1-x}Zn_xTe$ thin film at 'x' = 0.1865

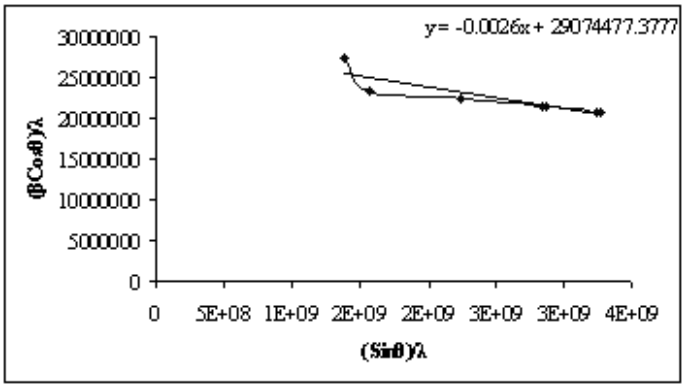

Fig. 2(b) Variation of (Sinθ)/λ vs (βCosθ)/λ of 100 nm $Cd_{1-x}Zn_xTe$ thin film at 'x' = 0.1865

Particle size is obtained from the intercept and strain is obtained from the slope of these plots. Particle size and strain are found to be 13.58 nm and -0.0146 respectively for $Cd_{1-x}Zn_xTe$ 1µm thin film at 'x' = 0.1865 and the particle size and strain are found to be 34.39 nm and -0.0026 respectively for $Cd_{1-x}Zn_xTe$ 100 nm thin film at 'x' = 0.1865. Similarly, for other values of 'x', particle sizes and strains are obtained. Variation of strain with particle size for all the compositions of $Cd_{1-x}Zn_xTe$ 1µm and 100 nm thin films are shown in Fig. 3(a) and Fig. 3(b) respectively.

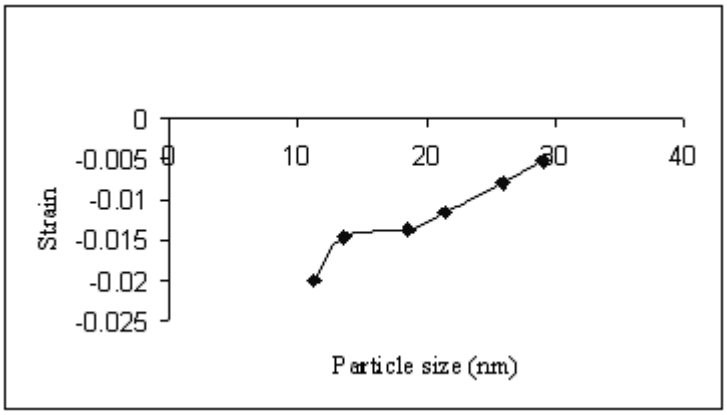

Fig. 3(a) Variation of strain with particle size for $Cd_{1-x}Zn_xTe$ 1µm thin films

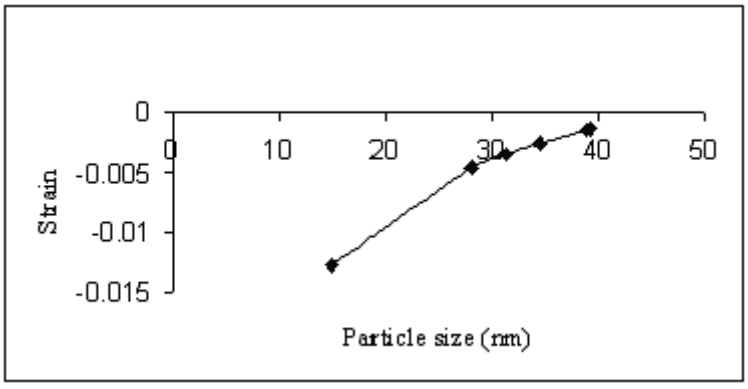

Fig. 3(b) Variation of strain with particle size for $Cd_{1-x}Zn_xTe$ 100 nm thin films

4. Discussions

In the X-Ray Diffraction (XRD) patterns of $Cd_{1-x}Zn_xTe$ 1µm and 100 nm thin films, for 'x' varying from 0.0567 to 0.2210, the peaks for CZT along with other peaks are identified. The peak heights and widths for identified planes are found to vary with 'x'. Some peaks are found to lie between those for CdTe and ZnTe as discussed in section 3 of this paper. Results obtained from XRD analysis indicate that 'x' is the parameter, in

controlling the structure of the films. It has been observed from Fig 1(a) and Fig. 1(b) that the values of peak-heights and peak-widths for identified planes in case of $Cd_{1-x}Zn_xTe$ 1µm thin film at 'x' = 0.1865 are more as compared to the values of these respective parameters for the respective planes in $Cd_{1-x}Zn_xTe$ 100 nm thin film at 'x' = 0.1865. Similar observation is found for other values of 'x'. This indicates that film thickness has good correlations to the heights and widths of XRD peaks. From the plots as shown in Fig. 1(a) and Fig. 1(b), it appears that the growth of $Cd_{1-x}Zn_xTe$ 1µm thin film at 'x' = 0.1865 is more crystalline than $Cd_{1-x}Zn_xTe$ 100 nm thin film at 'x' = 0.1865. Similar observation is obtained for other values of 'x'. This may be due to the greater impact of two-dimensional effect on $Cd_{1-x}Zn_xTe$ 1µm thin films over 100 nm thin films. Particle size and strain are obtained for $Cd_{1-x}Zn_xTe$ 1µm and 100 nm thin films as discussed in section 3.1 of this paper. It has been observed from Fig. 3(a) and Fig. 3(b) that with the decrease in the particle size, compressive strain increases. From the plots as shown in Fig. 1(a) and Fig. 1(b), it is observed that the sharpness of the identified peaks in the XRD spectra of $Cd_{1-x}Zn_xTe$ 100 nm thin film at 'x' = 0.1865 is less than those for $Cd_{1-x}Zn_xTe$ 1µm thin film at 'x' = 0.1865. Similar observation is obtained for other values of 'x'. This may be due to the predominance of nano-structured dimensional effect on $Cd_{1-x}Zn_xTe$ 100 nm thin films over $Cd_{1-x}Zn_xTe$ 1µm thin films. This indicates that film thickness has a good correlation to the sharpness of XRD peaks.

5. Conclusion

This study infers that dimensional effect has impact on structural properties of $Cd_{1-x}Zn_xTe$ thin films.

Acknowledgments

Author is thankful to all the members of Advanced Materials and Solar Photovoltaic Division, School of Energy Studies, Jadavpur University, Kolkata, India for their help and cooperation.

References

[1] J. P. Faurie, J. Reno and M. Boukerche J. Crystal Growth, 72, 1985, 111.
[2] R. Dornhaus, G. Nimitz, G. Höhler and E. A. Nickisch, Springer, 1983, 119.
[3] R. K. Willardson and A. C. Beer, Semiconductors and Semimetals, 13, 1978. Academic, New York.
[4] Z. Q. Shi, C. M. Stahle and P. Shu, Proc. SPIE, 90, 1998, 3553.
[5] T. E. Schlesinger, and R. B. James, Semiconductors and Semimetals, 43, 1995, Academic, San Diego.
[6] K. Guergouri, M. S. Ferah, R. Triboulet and Y. Marfaing, J. Cryst.Growth, 6, 1994, 139.
[7] Y. Eisen, I. Mardor, A. Shor et al., IEEE Trans. Nucl. Sci., 49, 2002, 172.
[8] H. Peng, P. D. Olcott, G. Pratx, A. M. K. Foudray, G. Chinn, C. S. Levin, IEEE Nuclear Science Symposium Conference Record, 2007.
[9] C. N. Brzymialkiewicz, M. P. Tornai, R. L. McKinley and J. E. Bowsher, IEEE Transactions on Medical Imaging, 24, 2005, 7.
[10] T. E. Schlesinger, J. E. Toney, H. Yoon, E. Y. Lee, B. A. Brunett, L. Franks and R. B. James, Material Science and Engineering 32, 2001, 103.
[11] K. P. Rao, O. Md. Hussain, K. T. R. Reddy, P. S. Reddy, S. Uthanna, B. S. Naidu. and P. J. Reddy, Journal of Alloys and Compounds, 218, 1995, p-86.
[12] D. Patidar, K. S. Rathore, N. S. Saxena, K. Sharma and T. P. Sharma, Chalcogenide Letters 5, 2008, 21.
[13] B. Samanta, S. L. Sharma and A. K. Chaudhuri, Vacuum, 46, 1995, 739.
[14] M. Li and J. C. Li, Materials Letters, 60, 2006, 2526.
[15] A. Nag, S. Sapra, S. Sen Gupta, A. Prakash, A. Ghangrekar, N. Periasamy, D. D. Sarma, Bull. Mater. Sci., 31, 2008, 561.
[16] C. N. R. Rao, G. U. Kulkarni, P. J. Thomas and P. P. Edwards, Chem. Eur. J 8, 2002, 29.
[17] S. Herrera, C. M. Ramos, R. Patino, J. L. Pena, W. Cauich, A. I. Oliva, Brazilian Journal of Physics, 36, 2006.
[18] J. L. Reno. and E. D. Jones, Phys. Rev. 45, 1992, 1440.
[19] M. Chakraborty, International Journal of Engineering Science and Technology, 3, 5, 2011,3798-3806.
[20] M. Chakraborty, International Journal of Engineering Science and Technology, 3,10, 2011, 7402-7407.
[21] Weblink: http://www.freepatentsonline.com/5528495.
[22] J. Pal, PhD Thesis, Jadavpur University, Kolkata, India, 2005.
[23] S. B. Quadri, E. F. Skelton, D. Hsu, A. D. Dinsmore, J. Yang, H. F. Gray and B. R. Ratna, Phys. Rev. B 60, 1999, 9191.
[24] A. R. Denton and N. W. Ashcroft, Physical Review A, 43, 1991, 3161.
[25] C. Kittel, Introduction to Solid State Physics, John Willey & Sons, 7th ed, 1996.